IOP Conference Series: Materials Science and Engineering

PAPER • **OPEN ACCESS**

Surface morphology and physicochemical properties of ordered mesoporous silica SBA-15 synthesized at low temperature

To cite this article: M H Koh *et al* 2017 *IOP Conf. Ser.: Mater. Sci. Eng.* **206** 012056

IOP Conf. Series: Materials Science and Engineering **206** (2017) 012056 doi:10.1088/1757-899X/206/1/012056

Surface morphology and physicochemical properties of ordered mesoporous silica SBA-15 synthesized at low temperature

M H Koh, S A Haji Azaman, B H Hameed, A T Mohd Din*

School of Chemical Engineering, Engineering Campus, Universiti Sains Malaysia, 14300 Nibong Tebal, Pulau Pinang, Malaysia.

*E-mail: chazam@usm.my

Abstract. The effects of process parameters on the surface morphology and physicochemical characteristics of ordered mesoporous silica SBA-15 synthesized at low temperature have been investigated in this study. SBA-15 particles were synthesized through sol-gel method using non-ionic surfactant Pluronic P123 and TEOS as a silica source with aqueous hydrochloric acid (HCl) as a catalyst under the following conditions: HCl concentration (1.0-2.5 M), ageing temperature (40-70ºC) and ageing time (12-48 hours). A series of physicochemical characterizations and material analyses were performed on SBA-15 particles including Scanning Electron Microscopy (SEM), Energy Dispersive X-ray Spectroscopy (EDX), Transmission Electron Microscopy (TEM), BET surface area analysis, Fourier transform infrared (FTIR) analysis and X-ray Diffraction (XRD) analysis. From the experimental observation, the conditions of HCl concentration, ageing temperature and ageing time were able to influence the surface morphology of SBA-15 particles. The presence of the ordered structures in SBA-15 particles was observed through the formation of 1-D cylindrical channels and 2-D hexagonal pores, inspected by using TEM. The detected XRD peak at (100) reflection signified the presence of ordered meso structures within the SBA-15 particles. Therefore, synthesis of SBA-15 particles through sol-gel method at low temperature is feasible and more sustainable if compared to the energy intensive hydrothermal method.

1. Introduction

Porous materials are defined as a continuous and solid network material filled with voids [1]. In the past few decades, demand on the usage of advanced structural materials has led to abundance of research carried out on porous solids such as porous carbon, synthetic silicate zeolites, mesoporous silicates and ordered porous metal oxides [2]. According to the International Union of Pure and Applied Chemistry (IUPAC), porous materials can be classified into three major classes based on their pore diameter sizes (d), microporous $d < 2$ nm, mesoporous $2 \leq d \leq 50$ nm and macroporous $d > 50$ nm. Microporous materials such as zeolites and metal-inorganic frameworks possess good stability, selectivity and activity due to their crystallinity and the presence of incorporated hetero elements in the structure. However, size limitation is a problem when it comes to large molecular application using microporous materials [3].

In 1972, Mobil Corporation explored the conversion of methanol into gasoline using microporous Zeolite ZSM-5 (Zeolite Socony Mobil) to obtain cheaper gasoline from acid-base reactions taking place within the micropores of zeolites [4]. However, this approach failed due to the fact that zeolite pore size was too small to enable the entry of larger organic molecules and for reactions to take place. Due to its size limitation, porous solids industry moved on to explore the possibility for mesoporous materials as substitutes to the microporous zeolites.

Generally, mesoporous materials possess high surface area of 400 – 1000 m^2 /g, large pore volume and excellent thermal stability at 500 – 600°C. Mesoporous solids can be prepared either by soft template or hard template method, in which organic molecules act as surfactant in soft template technique, while porous solids such as porous carbon is used in place of surfactant in hard template technique [1]. Mesoporous materials are highly favourable in large-molecular applications, such as cracking of heavy oil, polymer separation, enzyme immobilization and controlled-release of drugs [5].

The call for synthesis of ordered mesoporous materials stems from the fact that these materials consist of well-defined structural features such as pore sizes, pore shapes, pore arrangement and connectivity, which can be precisely-controlled by its synthetic conditions [5]. In fact, ordered mesoporous materials possess better hydrothermal stability, mechanical stability and catalytic activity in comparison to the disordered mesoporous materials [6]. Ordered mesoporous materials exhibit distinct, ordered-arrays of mesoporous channels in TEM images. Examples of ordered mesoporous materials are ordered metal oxides, ordered mesoporous silica, ordered mesoporous carbon, carbon nanotubes and mesoporous anodic alumina [7-8].

Ordered mesoporous silica SBA-15 has tunable pore size through modification on its synthesis parameters. A wide variety of SBA-15 morphologies has been reported in literature; including rods, fibers, spheres, gyroids, discoid-like and doughnut-like shape. Spherical hollow silica with porous shell finds great usage in controlled delivery of biomedical materials. They allow higher loading capacity to encapsulate drugs, genes or biological molecules in the shell [9]. Sakamoto and co-researchers reported a successful synthesis of rod-shaped SBA-15 in acidic media using Pluronic P123 as surfactant and tetramethyl orthosilicate as silica source; to give better adsorption of enzymes than the spherical SBA-15 particles [10].

There are various methods to synthesize SBA-15 including direct synthesis, synthetic grafting and impregnation, sol gel and immobilization. For direct synthesis method, it involves the reaction between co-condensation of silica source and silane groups or with different groups of metal such as transition, alkaline earth, rare earth and poor metals. Post grafting technique is the reaction between organosilane with silanol groups to produce covalent attachment of functional groups on surface of material using solvent under reflux condition [11]. Sol-gel is one of the methods that have been widely investigated in materials science. Orderly pore structure, size and shape of the SBA-15 can be achieved through this simple method [12]. Another advantage is the availability of high purity raw materials to support sol gel method [13]. This approach provides an important pathway to synthesize porous silica without requiring extremely high temperature as compared to the conventional hydrothermal treatment that requires high temperature [12]. For that reason, synthesis of SBA-15 particles through sol-gel method at low temperature is more sustainable.

In this work, SBA-15 was prepared by varying process parameters including ageing temperature, ageing time and HCl concentration, using sol-gel method. The surface morphology and physicochemical properties of SBA-15 prepared under low ageing temperature will be assessed in detail.

2. Materials and methods

2.1. Synthesis of SBA-15

The chemicals used in this work include Pluronic P123 ($PEO_{20}PPO_{70}PEO_{20}$) as surfactant, a silica source tetraethyl orthosilicate (TEOS)(98 %), and aqueous hydrochloric acid (HCl) were purchased from Sigma-Aldrich (Malaysia), Acros Organics (Malaysia), and R & M Chemicals (Malaysia), respectively. 150 mL of 2.5 M HCl was prepared and mixed with 5 g of Pluronic P123 in a beaker.

The mixture was then stirred until a colourless solution formed. At this point, 9.67 g of tetraethyl orthosilicate (TEOS) was added dropwise into the solution. The mixture was then stirred again for another 2 h until a white solution was formed. This mixture was left for ageing in a water bath shaker for 48 h at ageing temperature of 40 °C. White precipitate is filtered out and washed continuously with deionized water. The filtered white solid was then left for natural drying before calcination was carried out at 550°C for 4 h with heating rate of 5 °C/min. Subsequent trials were carried out at different synthesis conditions through one-variable-at-time (OVAT) approach summarized in Table 1. Samples 3, 5 and 9 are the replication points representing the maximum MB uptake capacity, respectively. Variation on other parameters such as surfactant and precursor concentration ratio, types of surfactant or precursor, calcination temperature etc, are not carried out, and these parameters remain constant whenever applicable.

Table 1. SBA-15 synthesis conditions.

Sample	[HCl] (M)	Ageing Temp (°C)	Ageing Time (h)
1	1.0	40	48
2	1.5	40	48
3*	2.0	40	48
4	2.5	40	48
5*	2.0	40	48
6	2.0	50	48
7	2.0	60	48
8	2.0	70	48
9	2.0	40	12
10	2.0	40	24
11	2.0	40	36
12*	2.0	40	48

*Synthesis under similar conditions.

2.2. Adsorption Test

A simple methylene blue (MB) adsorption test was carried out on the SBA-15 samples to determine the maximum MB uptake capacity (mg MB/g adsorbent). A mass of 0.1 g SBA-15 was added to 100 ml MB solution (100 ppm) and left for 48 h to achieve equilibrium. The MB concentration was analyzed using UV-Vis spectrophotometer (Shimadzu UV1800, Japan).

2.3. Materials Characterizations

Surface area properties of SBA-15 was determined using surface area analyser (Micrometrics ASAP 2010, USA) at 77 K. SEM with EDX analysis (SEM Quanta FEG 450, USA) was used to study surface topology of SBA-15 and textural images were captured using TEM (Philips TEM CM12, The Netherlands) Surface chemistry of SBA-15 and the crystal structure of SBA-15 are determined using FTIR spectrophotometer (Shimadzu IRPrestige-21, Japan) and Materials Research Diffractometer, respectively.

3. Results and discussion

The surface morphology of SBA-15 synthesized at different HCl concentrations are shown in Figure 1. The formation of SBA-15 rods and spherical-shaped particles can be observed at 1.0 M HCl, evolving from shorter rods (2.0 M, 1.5 M) to longer rectangular rods (2.5 M), with increasing HCl concentrations. This is evidenced that the particle shape of SBA-15 can be greatly influenced by the addition of different HCl concentrations. This can be explained by colloidal phase separation mechanism (CPSM) proposed by Zhao and co-workers [14]. The theory suggests that when phase separation occurs, precipitates will be observed in the solution and the rate of this phase separation affects the final morphology of ordered mesoporous structures. Besides, it is better to synthesize SBA-

15 at highly acidic condition when using TEOS as a silica source. Xiao Ying and co-researchers studied the effect of HCl concentration using three different silica sources: 1,2-bis(trimethoxysilyl)ethane (BTMSE), 1,2-bis(triethoxysilyl)ethane (BTESE) and tetraethyl orthosilicate (TEOS), all accompanied by the same surfactant, Pluronic P123. The results shown that organosilica precursor (BTMSE/ BTESE) interacts poorly with surfactant and condenses faster than the silica precursor such as TEOS. Since hydrochloric acid acts as a catalyst to improve hydrolysis and condensation rate of the precursors, high acid concentration leads to rapid condensation of organosilica framework, which results in poorly defined pores. Lowering the acid concentration has proven to reduce the condensation rate of BTMSE and BTESE and only then a well-defined hexagonal pore arrangement in SBA-15 could be obtained. In contrast to the synthesis using TEOS, condensation happens very slowly in aqueous solution and high acid concentration is generally required to increase the condensation rate of silicate framework [15]. In another study, a formation of rod-shaped SBA-15 particles prepared using TEOS at different HCl concentrations without the use of any additives has been previously observed [16]. It was reported that there was no significant differences in the rod-shaped and length of SBA-15 synthesized at 2.0 M HCl, which is consistent to the current observation in Figure 1(c).

Figure 2 shows the surface morphology of SBA-15 synthesized at different ageing temperatures of 40, 50, 60 and 70°C, using 2.0 M HCl and ageing time of 48 h. It is observed that as the ageing temperature increases, the shape of SBA-15 particles changes from short rods (40 and 50°C) to thinner fibre-like structure (60 and 70°C). This phenomenon can be explained using the CPSM theory. Free energy of mesostructure self-assembly (ΔG), dominantly affects the final morphology of SBA-15. As mesostructure is continuously being formed, to minimize ΔG, more crystal-like structures of SBA-15 can be obtained. In this work, SBA-15 particles tend to take up fibre-like structure at 60 and 70ºC. The average length and width were measured at 700 nm and 500 nm for the SBA-15 sample prepared at ageing temperature of 40°C. SBA-15 is commonly formed by grains of relatively uniform size; typically in the range of 300–500 nm (width) and 700–1000 nm (length) [17]. A previous study has reported the average particle length and width of 800 nm and 500 nm, respectively for the SBA-15 synthesized at 35°C, 2.0 M HCl and ageing time of 10 h [16].

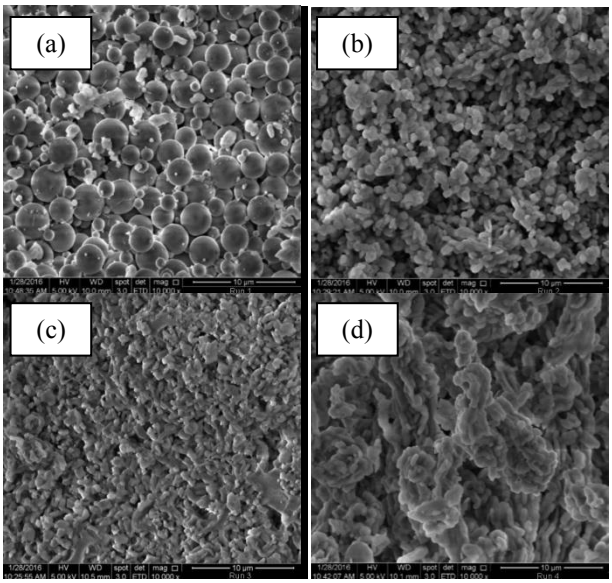

Figure 1. Surface morphology of SBA-15 synthesized at different HCl concentrations; (a) 1.0 M (b) 1.5 M (c) 2.0 M and (d) 2.5 M (×10k magnification).

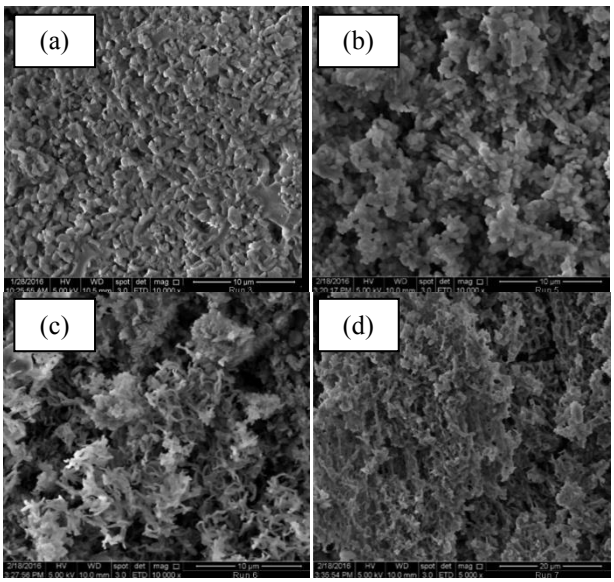

Figure 2. Surface morphology of SBA-15 synthesized at different ageing temperature; (a) 40°C (b) 50°C (c) 60°C and (d) 70°C (×10k magnification).

Figure 3 shows surface morphology of SBA-15 prepared at different ageing times of 12, 24, 36 and 48 h (HCl concentration: 2.0 M, ageing temperature: 40°C). From the images, it is evidence that the surface morphology of SBA-15 can be influenced by the ageing time parameter. The SBA-15 particles prepared at 12 and 24 h ageing times were random in size and not uniform in shape. More well-defined short rod-shape SBA-15 particles are noticed when ageing time is increased to 36 and 48 h. This could be explained since longer ageing time has allowed more polymerization and condensation of silica species on the walls to form ordered mesostructure of SBA-15 [18].

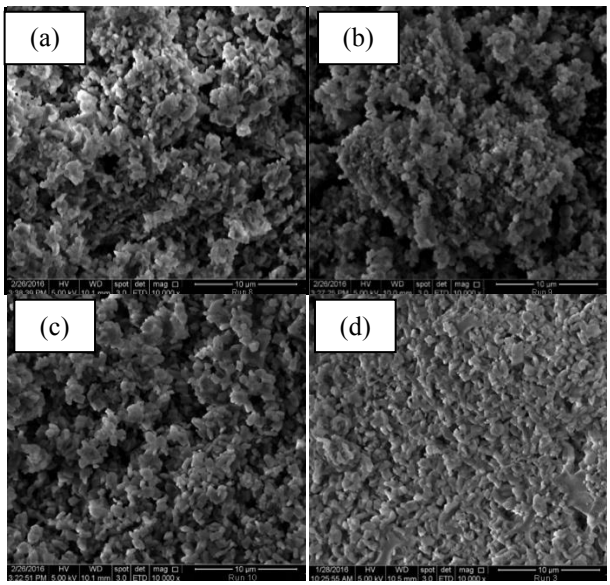

Figure 3. Surface morphology of SBA-15 synthesized at different ageing time; (a) 12 h (b) 24 h (c) 36 h (d) 48 h (×10k magnification).

A similar observation has also been recorded in our previous work [19]. However, a shorter ageing time is not unusual [20]. An investigation on the effect of ageing time on the mesoscopical order and pore structure of functionalized mesoporous silica SBA-15 has shown that longer ageing time has contributed to a better ordered pore structure formation [18].

A simple MB adsorption test was performed to select the SBA-15 sample with the highest MB uptake capacity. MB adsorption test is a common method to determine the mesoporosity attribute of a porous solid. Maximum MB uptake capacities for all the SBA-15 samples, synthesized in this study are summarized in Table 2. It was found out that sample 3, prepared under the respective conditions: 2.0 M HCL, 40°C and 48 h ageing time, has exhibited the highest MB uptake of 196.3 mg MB/g adsorbent. Hence, sample 3 SBA-15 has been selected for further physicochemical analyses.

Figure 4 shows the textural imaging of sample 3 SBA-15. From the TEM images, 1-D cylindrical hollow channels and 2-D hexagonal pore arrangement can be clearly observed, a common attribute for SBA-15. The hollow channels were measured at 2.5 nm in width. The value is smaller to a measurement of 5 nm in width for hollow channels of SBA-15 prepared through hydrothermal treatment at 80°C [17]. Hydrothermal method normally requires the process to be sustained at temperature ranging from 80 - 120 ºC, which means more energy utilization [12].

Table 2. Maximum MB uptake capacity.

Sample	MB uptake capacity (mg/g)
1	113.6
2	99.6
3*	196.3
4	132.7
5*	196.3
6	58.9
7	36.1
8	2.60
9	99.0
10	95.1
11	35.7
12*	196.3

*Synthesis under similar conditions.

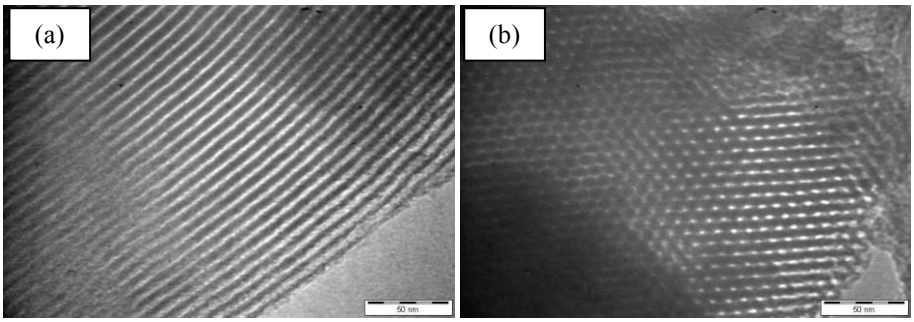

Figure 4. TEM images of Sample 3 SBA-15 (a) cross-sectional view and (b) perpendicular to pore channels.

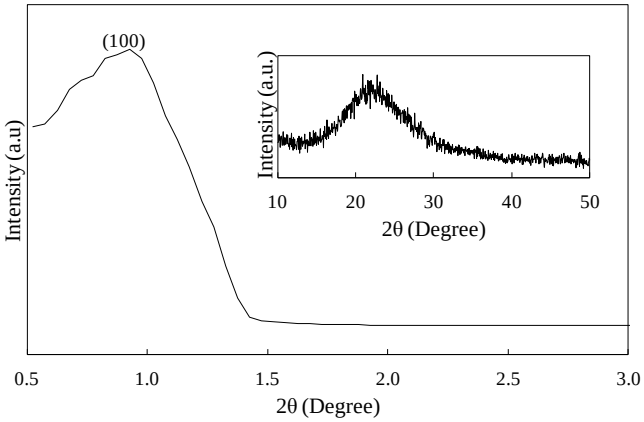

Figure 5. XRD pattern for Sample 3 SBA-15.

Figure 5 shows the XRD profile for Sample 3 SBA-15. At low angle, a well-resolved diffraction peak is detected corresponding to the Miller index (100) reflection around 1° point. This peak is a characteristic of 2-D hexagonal pore arrangement, a typical signature for SBA-15 material.

2-D hexagonal symmetry structure (p6mm) corresponding to (110) and (200) reflections are not detected in the XRD profile. Unit cell parameter, a_o, is calculated at 10.88 nm based on the first Bragg peak position, d_{100} = 9.42 nm. The wall thickness, w_t, of SBA-15 is measured at 6.98 nm. The formation of distintive peak between 20-25° represents the amorphous nature of the synthesized siliceous material (Figure 5 - inset).

The EDX spectra (Figure 6) shows the respective weight percentage contributed by each element in SBA-15 sample. The weight percent for carbon, silica and oxygen are given at 8.33 % (C), 58 % (Si) and 33.67 % (O), respectively. The intensity of the detected peaks for Si and O elements is comparable to the literature findings [21].

From Figure 7, a strong broad peak observed at 1094 cm^{-1} can be assigned to siloxane bond (-Si-O-Si-) stretch. -OH stretching vibrations mode of the silanol groups involved in hydrogen interactions with the adsorbed water molecules is observed at 3454 cm^{-1} peak. Bending H_2O band at 1637 cm^{-1} is also ascribed to the adsorbed water molecules on the material. The presence of these two functional groups confirmed the silica formation. Another obvious band at around 802 cm^{-1} can be ascribed to symmetric stretching from -Si-O bonds, while another peak at around 466 cm^{-1} can be attributed to bending of -Si-O-Si- bonds [22]. The absence of peaks at 3000-2850 cm^{-1} range (-CH_2- stretching) and 1470-1450 cm^{-1} (-CH_2- bending) confirmed the complete removal of Pluronic P123 in SBA-15 sample [20].

Figure 8 shows the nitrogen adsorption-desorption isotherm performed on Sample 3 SBA-15 at 77K. The respective sample exhibits Type IV adsorption isotherm with H1-type hysteresis loop. H1 is commonly associated with porous materials exhibiting cylindrical-like pores [23]. It has been observed from literature that the well-formed SBA-15 always shows Type IV adsorption isotherm with H1-type hysteresis loop [17]. Due to the capillary condensation process in hysteresis loop region, larger pressure drop is required during desorption in order to overcome the van der Waals interactions among the adsorbed liquid molecules in the confined pores or capillaries. This is a typical phenomenon observed for adsorption-desorption isotherm of mesoporous materials [24].

The steep increase of N_2 adsorption at P/Po = 0.52 indicates the mesopore uniformity. This is highly consistent with the Barret-Joyner-Haleda (BJH) pore size distribution plot (figure is not shown) having a sharp peak at pore diameter of 4.06 nm [15]. The average pore size was measured at 3.90 nm based on the BET adsorption branch. The total pore volume, V_{Total}, and micropore volume, V_{μ}, for this sample are 0.36 and 0.021 cm^3/g, respectively. Total BET surface area is calculated at 364 .71 m^2/g.

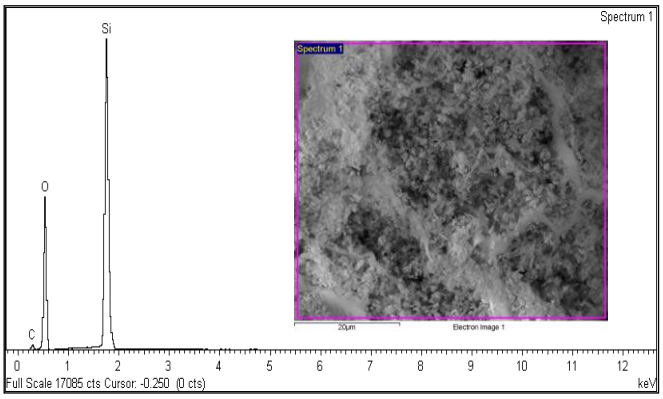

Figure 6. EDX spectra of of Sample 3 SBA-15.

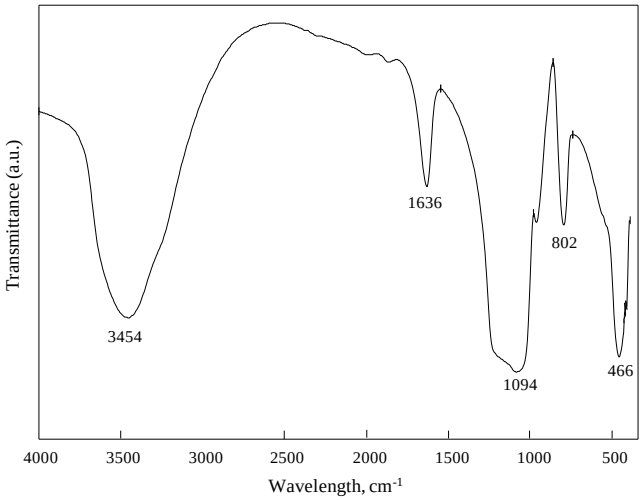

Figure 7. FTIR spectra of Sample 3 SBA-15.

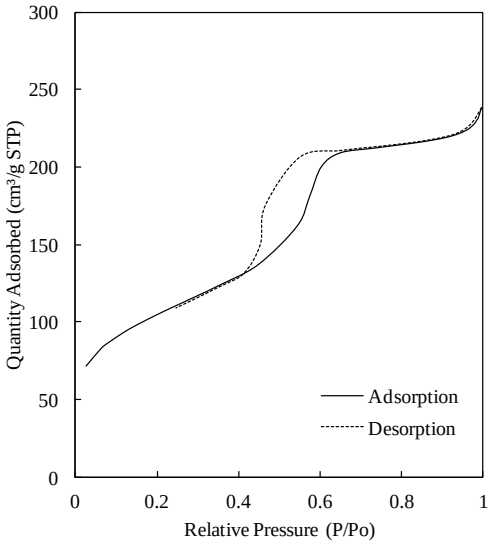

Figure 8. Nitrogen adsorption-desorption isotherm of Sample 3 SBA-15 at 77K.

4. Conclusions

Ordered mesoporous silica SBA-15 has been successfully synthesised in this present work. At lower HCl concentrations, the synthesized SBA-15 particles tend to form a spherical shaped; while at higher HCl concentration range, a rod-like shape nanoparticles were observed. Ageing temperature and ageing time also have been found to influence the shape of SBA-15 particles. Upon increasing the ageing temperature from 40 to 70°C, SBA-15 changed from short rods to thin-fibre like structure. The presence of the ordered structures in SBA-15 sample was observed through the formation of 1-D cylindrical channel and 2-D hexagonal pores, inspected using TEM. The results were further validated with the detected XRD peak at (100) reflection; a sign of ordered meso structures formation in SBA-15 particles.

Acknowledgements

The authors are thankful to Universiti Sains Malaysia and Ministry of Higher Education, Malaysia (MOHE) for providing research facilities and financial support for this research. This research is funded by MOHE under the Fundamental Research Grant Scheme (FRGS - Project number: 6071330).

References

[1] Pal N and Bhaumik A 2013 Soft templating strategies for the synthesis of mesoporous materials: inorganic, organic-inorganic hybrid and purely organic solids *Adv. Colloid. Interface. Sci.* **189-190** 21-41

[2] Mejia E E 2013 *Characterization of Some Natural and Synthetic Materials with Silicate Structures* (Sweden:Universitetstryckeriet, Luleå)

[3] Buckley R W and Benito P 2007 *Solid State Chemistry Research Trends* (Nova Science Publishers) pp 173-225

[4] Vallet-Regí M 2012 Mesoporous Silica Nanoparticles: Their Projection in Nanomedicine *ISRN. Mat. Sci.* **2012** 1-20

[5] Zhang Q and Wei F 2014 *Adv. Hierar. Nanostruct. Mat.* (Wiley) p 512

[6] Bonneviot L, Béland F, Danumah C, Giasson S and Kaliaguine S 1998 *Mesoporous Molecular Sieves* (Elsevier Science) p 614

[7] Nhut J M, Pesant L, Tessonnier J P, Winé G, Guille J, Pham-Huu C and Ledoux M J 2003 Mesoporous carbon nanotubes for use as support in catalysis and as nanosized reactors for one-dimensional inorganic material synthesis *App. Catalysis A: General.* **254** 345-363

[8] Bruschi L, Mistura G, Park S J and Lee W 2014 Adsorption of argon onmesoporous anodic alumina *Adsorption.* **20** 889-897

[9] Prokopovich P 2015 *Biological and Pharmaceutical Applications of Nanomaterials* (CRC Press) p 444

[10] Sakamoto Y, Kaneda M, Terasaki O, Zhao D Y, Kim J M, STucky G, Shin H J and Ryoo R 2000 Direct imaging of the pores and cages of three dimensional mesoporous materials *Nature*. 449-453

[11] Rahmat N, Abdullah A Z and Mohamed A R 2010 A review: Mesoporous Santa Barbara amorphous-15, types, synthesis and its applications towards biorefinery production *Am. J. Appl. Sci.* **7** 86-1579

[12] Rivera-Muñoz E M and Huirache-Acuña R 2010 Sol Gel-derived SBA-16 mesoporous material *Int. J. Mol. Sci.* **11** 86-3096

[13] AlOthman Z A 2012 A review: Fundamental aspects of silicate mesoporous materials. *Materials. (Basel).* **5** 2874–2874

[14] Zhao D, Wan Y and Zhou W 2012 *Ordered Mesoporous Mat.* (Weiheim: Wiley)

[15] Xiao Ying B, X S Z, Xu L, Pai Ann C and Jun L 2004 A Novel Route toward the Synthesis of High-Quality Large-Pore Periodic Mesoporous Organosilicas *J. Phys. Chem. B.* **108** 4684-4689

[16] Wang Y, Zhang F, Wang Y, Ren J, Li C, Liu X, Guo, Y, Guo Y and Lu G 2009 Synthesis of

length controllable mesoporous SBA-15 rods *Mat. Che. and Phy..* **115** 649-655
[17] Klimova T, Esquivel A, Reyes J, Rubio M, Bokhimi X and Aracil J 2006 Factorial design for the evaluation of the influence of synthesis parameters upon the textural and structural properties of SBA-15 ordered materials *Microporous and Mesoporous Mat.* **93** 331-343
[18] Wei Q, Hao Z N Y, Liu L and Zou Z C J 2006 Effect of synthesis conditions on the mesoscopical order of mesoporous silica SBA-15 functionalized by amino groups *J. Sol-Gel. Sci. Techn*. **39** 9-103
[19] Mohd Din A T, Ahmad M A and Hameed B H 2015 Ordered mesoporous carbons originated from non-edible polyethylene glycol 400 (PEG-400) for chloramphenicol antibiotic recovery from liquid phase *Chem. Eng. J.* **260** 730-739
[20] Gandhi S, Sethuraman S and Krishnan U M 2013 Heterogeneous mesoporous SBA-15 silica as catalyst towards the synthesis of various biodegradable aliphatic polyesters *Macromolecular. Res.* **21** 833-842
[21] Tomer V K, Duhan S, Adhyapak P V, Mulla I S and Gouma P 2015 Mn-Loaded Mesoporous Silica Nanocomposite: A Highly Efficient Humidity Sensor *J. American Ceramic Soc..* **98** 741-747
[22] Yang L, Jiang Z, Lai S, Jiang C and Zhong H 2014 Synthesis of Titanium Containing SBA-15 and Its Application for Photocatalytic Degradation of Phenol *Int. J. Chem. Eng.* **2014** 1-7
[23] Thommes M 2010 Physical adsorption characterization of nanoporous materials *Chemie-Ingenieur-Technik.* **82** 73-1059
[24] Naumov S 2009 *Hysteresis Phenomena in Mesoporous Mat* (Leipzig, Leipzig University)